ANTICANCER RESEARCH *40*: 2591-2599 (2020)
doi:10.21873/anticanres.14230

The Application of a Low-temperature Physical Plasma Device Operating Under Atmospheric Pressure Leads to the Production of Toxic NO_2

KARSTEN KLETSCHKUS[1], LYUBOMIR HARALAMBIEV[2,3], ANDREAS NITSCH[2], FELIX PFISTER[4], GERD KLINKMANN[5], AXEL KRAMER[6], SANDER BEKESCHUS[7], ALEXANDER MUSTEA[4] and MATTHIAS B. STOPE[1,4]

[1]*Plasma Oncology Laboratory, Department of Urology, University Medicine Greifswald, Greifswald, Germany;*
[2]*Department of Trauma, Reconstructive Surgery and Rehabilitation Medicine, University Medicine Greifswald, Greifswald, Germany;*
[3]*Department of Trauma and Orthopaedic Surgery, BG Klinikum Unfallkrankenhaus Berlin GmbH, Berlin, Germany;*
[4]*Department of Gynecology and Gynecological Oncology, University Hospital Bonn, Bonn, Germany;*
[5]*Department of Anesthesiology and Intensive Care Medicine, University Medical Center Rostock, Rostock, Germany;*
[6]*Institute of Hygiene and Environmental Medicine, University Medicine Greifswald, Greifswald, Germany;*
[7]*ZIK plasmatis, Leibniz Institute for Plasma Science and Technology (INP Greifswald), Greifswald, Germany*

Abstract. *Background: Physical plasma is a mixture of reactive particles and electromagnetic radiation. Due to the antimicrobial, immunomodulatory, anti-inflammatory, wound-healing promoting, and antineoplastic effects of body tempered physical plasma under atmospheric pressure (cold atmospheric plasma: CAP), CAP therapy is increasingly becoming the focus of surgical and oncological disciplines. However, when applied in practice, a potential emission of harmful noxae such as toxic nitrogen oxides must be taken into account, which was investigated in the following study. Materials and Methods: MiniJet-R Ar CAP device was characterized with respect to NO_X-specific spectra, ultraviolet radiation C (UVC) intensity in the range of 200-275 nm and the formation of NO_X gases. Instrument-specific parameters such as gas flow, energy setting of the high-frequency generator, and flow rate of the carrier gas Ar were varied. To test the toxic properties of the NO_2 concentrations formed by CAP, SK-OV-3 human ovarian cancer cells were incubated with different NO_2 concentrations and cell growth was monitored for 120 h. Results: The operation of MiniJet-R led to the formation of NO_2 in the proximity of the CAP effluent. Synthesis of NO led to a NO-specific spectrum in the range of 100-275 nm, whereby UVC radiation produced reached intensities of up to 90 mW/m^2. NO gas itself, however, was not detectable, as it was converted to NO_2 rapidly. Cell culture incubation experiments demonstrated that NO_2 in these concentration ranges had no influence on the cell growth of human cancer cells. Conclusion: Although no limit values were exceeded in the present study, the emission of high-energy UVC radiation and toxic NO_2 is a risk factor with regard to the legal regulations on workplace protection (operator hazard) and the approval of medical devices (patient hazard). This is important for considerations regarding treatment frequency and duration. The growth inhibitory effect of CAP treatment on human cancer cells principally suggests a medical application of the MiniJet-R device, although more extensive studies will have to follow.*

Correspondence to: Matthias Stope, Department of Gynecolgy and Gynecological Oncology, University Hospital Bonn, Venusberg-Campus 1, 53127 Bonn, Germany. Tel: +49 22828711361, Fax: +49 22828716091, e-mail: matthias.stope@ukbonn.de

Key Words: Physical plasma, cold atmospheric plasma, plasma medicine, radiation, nitrogen oxides, occupational health and safety.

Physical plasma is a mixture of particles of a carrier gas and ambient air with different ionization and excitation states, as well as electromagnetic radiation of different wavelengths including ultraviolet radiation C (UVC). In medical applications, body-tempered ('cold') plasmas up to about 40˚C under normal atmospheric pressure (cold atmospheric plasma: CAP) are utilized (1, 2). CAP has antimicrobial, immunomodulating, anti-inflammatory, wound-healing promoting, and antineoplastic effects on biological tissue and is therefore tested for its applicability in various medical fields. Due to the physical properties of CAP and against the

background of the equipment available for plasma generation, investigations into its medical application have so far been limited to the treatment of surfaces. The therapy of dental and skin diseases has been the main focus of research (3–5). In recent years, further applications have become the focus of interest, since the biological effects of CAP also make its application in surgical therapy, especially in oncological surgery, appear promising (6–9). In recent years, this has led to the development of the innovative research field of plasma medicine and thus also to the ongoing development of devices suitable for the production of CAP.

Devices for medical applications must comply with specifications that largely exclude the risk to both the treated patient and the operator. In the case of high-frequency (HF) devices such as CAP devices, the emission of electromagnetic radiation and gases formed under high-energy conditions is particularly relevant. The aim of this work was to investigate the CAP device MiniJet-R (Heuermann HF Technik, Aachen, Germany) for the formation of NO_X components. The device uses Ar as a carrier gas and generates CAP by employing a microwave HR generator. So far, this CAP device has only been used for technical applications. The present study is part of a comprehensive characterization of the CAP device with regard to its potential use in medicine. The focus is on the formation of toxic NO_X gases by CAP.

Materials and Methods

MiniJet-R CAP device. The MiniJet-R device from Heuermann HF Technik (Aachen, Germany) was used to produce CAP (Figure 1A and B). The CAP was generated by microwaves (2.48 GHz) in an HF generator with power up to 10 W. The carrier gas was Ar (purity 99.996%). The temperature of the generated CAP was slightly below 40˚C, and therefore suitable for medical applications without causing thermal effects on body tissue. The flow rate of the carrier gas argon and the power of the HF generator were adjustable.

To determine the Ar flow rate, a type 35810 gas flow meter (Analyt-MTC, Mülheim, Germany) was connected to the CAP instrument. A laminar flow element measured pressure differences in the flow rate in front of and behind the laminar flow element and the Ar-specific gas flow rate was calculated.

Setup of the measurements of UVC intensity in the range of 200-275 nm and NO_X concentrations were performed at different distances from the tip of the handpiece and at different angles to the longitudinal axis of handpiece and effluent (Figure 1C and D).

Spectral analysis. A Maya 2000Pro spectrometer (Ocean Insight, Orlando, FL, USA) was used for spectral measurement of the CAP effluent. The spectrometer was equipped with a UV-UPGD 2400 line grating and a 10 μm input port. A Hamamatsu S10420 photodetector was tuned for the range of 164-275 nm. The photoelectric detection of the radiation was performed on a semiconductor with 2,068 individual channels with a resolution of 0.05 nm.

For spectral analysis, the plasma handpiece was positioned directly in front of the entrance slit of the spectrometer, thus eliminating the need for focusing optics. To determine the angle dependence of the spectrum, the spectrometer was rotated by specified angles of 0˚, 30˚, 60˚, and 90˚. The data from the spectrometer were evaluated with Ocean View software (Ocean Insight).

Analysis of NO/NO_2. The measurement of NO and NO_2 was performed with an APNA 370 NO_X monitor (HORIBA Europe, Oberursel, Germany). The APNA 370 works according to the chemiluminescence principle. NO reacts with ozone in APNA 370 to form NO_2. A part of the NO_2 is in an excited state, which is decomposed by spontaneous photoemission. The measured intensity of the light emitted with a wavelength of 600-3,000 nm is proportional to the amount of NO in the gas sample. The NO_2 concentration is measured indirectly. NO_2 present in the sample is reduced to NO in a NO_X converter in APNA 370. and the NO_2 concentration of the gas sample results from the difference between the NO measurements.

The measuring range went up to a maximum of 1 μg/m^3 and was automatically switched to a maximum of 10 μg/m^3 when the range was exceeded. A suction hose (length 5 m, inner diameter 6 mm) was connected to the sample inlet of the instrument. The free end of the hose was installed 1 cm in front of the handpiece of the CAP instrument. Gas samples were aspirated at a flow rate of 0.8 l/min. The values given are cumulative measurements over 1 min. After each measurement, the CAP generator was switched off, the NO/NO_2 sensor was flushed with ambient air for a few minutes and the measurement was continued with a higher power level of the CAP device. In addition to the NO/NO_2 concentrations, the UVC intensity of the CAP effluent was also continuously recorded in parallel.

Specific analysis of NO_2. An I-55D gas sensor (IT Dr. Gambert, Wismar, Germany) was applied for the more sensitive detection of NO_2 alone. For the determination of the NO_2 background in the laboratory atmosphere, the NO_2 concentration was recorded over a period of 90 s without the operation of the CAP device using the I-55D gas sensor. For measurements during operation of the CAP device, the CAP effluent was directed to a UVC sensor (SUV 20.2 with MUV 2.4 WR reference radiometer, IL Metronic, Ilmenau, Germany) 11 mm away as a baffle. In an extension of the surface of the UVC sensor and at an angle of 40˚ to it, the tip of the suction cannula of the NO_2 gas sensor was placed at 10 cm, 20 cm, and 30 cm distance. A gas sample with a flow rate of 200 ml/min was fed to the sensor by a suction gas pump. The NO_2 concentration was recorded for 400 s.

Analysis of UVC intensity. To measure the UVC intensity, SUV 20.2 UVC sensor and the corresponding reference radiometer MUV 2.4 WR (sensitivity range of 220-280 nm; both IL Metronic) connected to a traceably calibrated and adjusted MUV 2.4 WR reference radiometer. The UVC sensor was placed in the longitudinal axis of the CAP effluent at a distance of 11 mm from the tip of the handpiece of the CAP instrument.

Cell culture incubation experiments. For treatment, SK-OV-3 human ovarian cancer cells (Cell Lines Service, Eppelheim, Germany) were treated with CAP (power level 5) in suspension (2×10^4 cells/300 μl) for 30 s or 60 s. The cell suspensions were then made up to 1,000 μl with cell culture medium of Dulbecco's modified Eagle's medium/F12 (Life Technologies, Darmstadt,

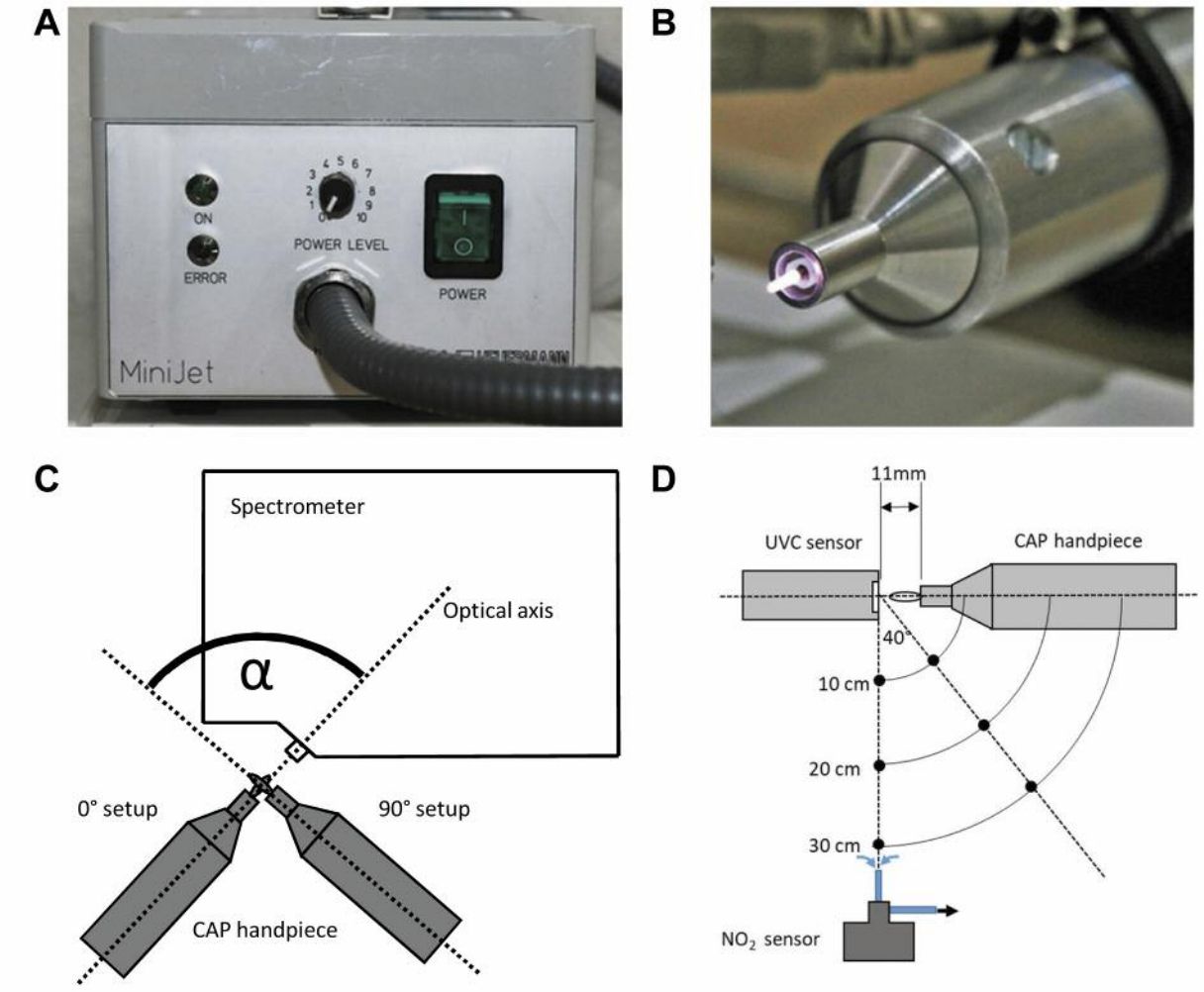

Figure 1. *MiniJet-R cold atmospheric plasma device from Heuermann HF Technik (Aachen, Germany). A: High-frequency generator including a power switch and a regulator for the power level. B: The tip of the handpiece with the cold atmospheric plasma effluent. C: Measurement setup for taking the spectrum in longitudinal direction (0˚) and transverse (90˚) to the axis of handpiece and plasma effluent. D: Measuring set-up for determining the NO_2 concentration at an angle of 90˚ and 40˚ to the axis of the handpiece and plasma effluent. The ultraviolet radiation C sensor served as a baffle. The measurements were performed at a distance of 10, 20, and 30 cm from the point of impact of the effluent.*

Germany) with 5% fetal bovine serum (Biochrom, Berlin, Germany), and 0.125% gentamicin (Ratiopharm, Ulm, Germany) and the complete 1,000 µl cell suspensions were seeded in 24-well cell culture plates. Cells treated with Ar gas alone instead of CAP were used as controls. Up to 120 h after treatment, cell counts were determined at 4, 24, 48, 72, 96, and 120 h using a CASY TT Cell Counter and Analyzer (Roche Applied Science, Mannheim, Germany). Cells were separated, 1:100 diluted in CASYton solution (Roche Applied Science) and 400 µl of each dilution and counted in triplicate using a 150 µm capillary (gate settings: 7.00 µm/15.15 µm).

To determine the impact of NO_2 on cell growth, SK-OV-3 cells were seeded in 24-well cell culture plates as decribed above and without CAP treatment, incubated for 120 h without and with 1.925 $\mu g/m^3$ NO_2, and the cell count was measured at the specified times as indicicated above.

Results

Spectral analysis for the UVC range was limited to the wavelength range of 200 nm to 275 nm, as radiation below 200 nm is absorbed under normal conditions by atmospheric oxygen and nitrogen. The observed UVC spectrum from 200 to 275 nm exhibited significant intensities above background noise. Six characteristic double peaks at 214.75±0.05/215.29±0.05 nm, 226.15±0.05/226.73±0.05 nm, 236.15±0.05/236.83±0.05 nm, 246.92±0.05/247.64±0.05 nm, 258.50±0.05/259.36±0.05 nm, and 271.08±0.05 nm/271.92±0.05 nm appeared (Figure 2). The spectrum maintained its characteristics independently of carrier gas flow rate (Figure 2A), HR generator power (levels 4 to 6; Figure 2B), and the angle to the longitudinal axis of the CAP

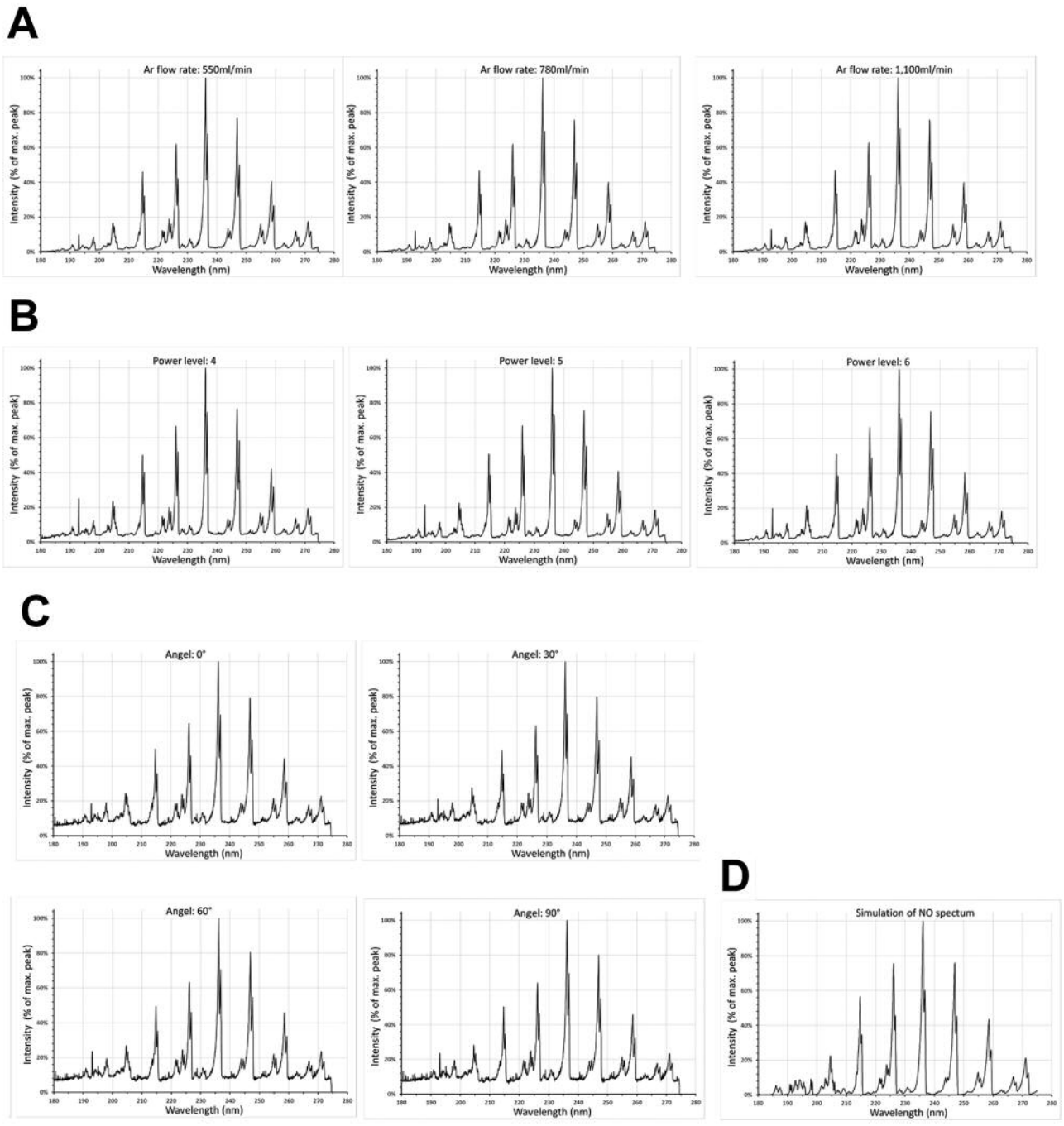

Figure 2. *Ultraviolet radiation C (UVC) intensity in the wavelength range of 180-275 nm produced by cold atmospheric plasma. Measurements were made with a UVC SUV 20.2 sensor coupled to a MUV 2.4 WR radiometer (both IL Metronic, Ilmenau, Germany) at a distance of 11 mm from the cold atmospheric plasma effluent at different Ar flow rates (A), power levels (B), and angles to the cold atmospheric plasma effluent (C). D: In-silico simulation of a NO spectrum generated with LIFBASE software (10).*

effluent (Figure 2C). Only the intensities of the double peaks varied marginally (data not shown), for which reason relative intensities are given in Figure 2 for better comparability. An *in silico* analysis of the spectrum with LIFBASE software developed for 2-atomic molecules (10) showed a spectrum almost identical to that for NO (Figure 2D). Based on this simulation, it can be assumed that the use of CAP led to the emission of NO.

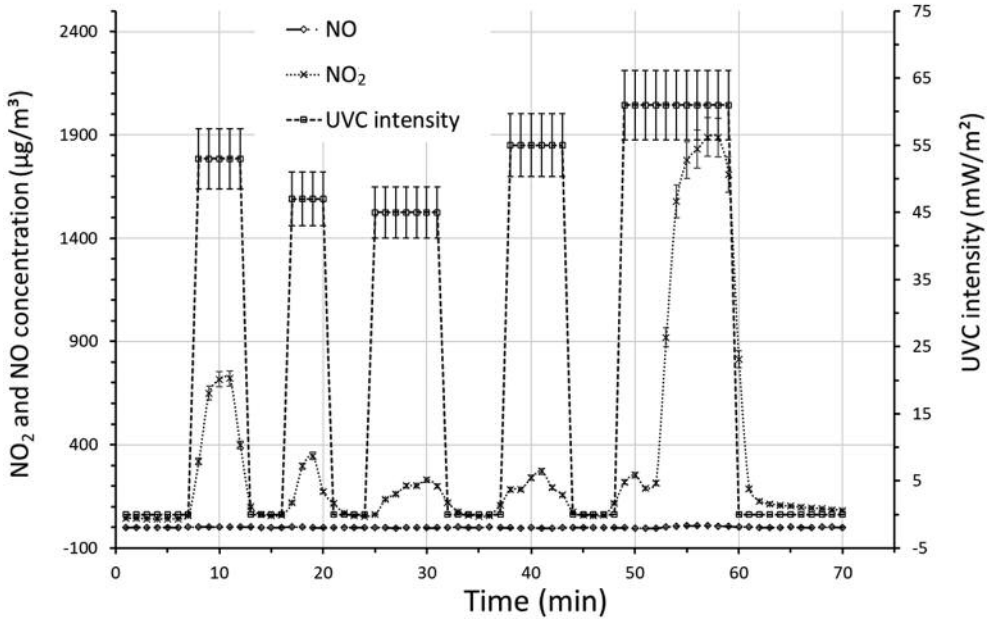

Figure 3. *Determination of NO and NO_2 concentrations with an APNA 370 NO_X monitor operated at power levels from 1 to 5 with simultaneous detection of ultraviolet radiation C (UVC) intensity in the range of 200-275 nm with SUV 20.2 sensor coupled to a MUV 2.4 WR radiometer. The data are given as average values with the device-specific errors as deviation.*

This hypothesis was tested in the state laboratory of the Berlin Air Quality Network with the APNA 370 NO_X monitor (HORIBA). The qualitative series of measurements allowed the verification of NO production and also a further investigation into the possible formation of NO_2. The monitoring of NO/NO_2 concentrations was performed continuously while the CAP device was operated at power levels from 1 to 5 for several minutes (Figure 3). Ambient air without the operation of the CAP device gave concentrations of 3±13 µg/m^3 NO and 38±13 µg/m^3 NO_2. During the operation of the CAP device over power levels of 1 to 5, the NO concentration did not change and remained below the limit of detection (power level 1: 3±13 µg/m^3 NO; power level 2: 3±13 µg/m^3 NO; power level 3: 0±13 µg/m^3 NO; power level 4: -1±13 µg/m^3 NO; power level 5: 8±13 µg/m^3 NO). The NO_2 concentration during CAP operation was much higher than the NO_2 content of ambient air and peaked at the highest power level (power level: 1: 230±20 µg/m^3 NO_2; 2: 340±20 µg/m^3 NO_2; 3: 320±20 µg/m^3 NO_2; 4: 270±20 µg/m^3 NO_2; 5: 1,900±20 µg/m^3 NO_2). Under the selected operating conditions the measured UVC intensities during CAP operation remained comparatively constant at 53±5 mW/m^2 (power level 1), 47±4 mW/m^2 (power level 2), 45±4 mW/m^2 (power level 3), 55±5 mW/m^2 (power level 4), and 61±5 mW/m^2 (power level 5).

Since NO was not detected during the operation of the CAP device, the following measurements were carried out with an I-55D gas sensor specific for NO_2 determination and much more sensitive. Continuous analysis of the environmental NO_2 over 100 s without CAP but with and without Ar flow showed relatively large variations in the background NO_2 concentration (Figure 4A). Cumulative values over the measurement period varied independently of the Ar flowing through the device, ranging from 8 to 20 µg/m^3 NO_2 without Ar flow and 7 to 20 µg/m^3 NO_2 with Ar.

During the operation of the CAP device, the formation of NO_2 was verified. The NO_2 formation rate remained constant at low Ar flow rates of 500 to 800 ml/min but then increased from 900 ml/min and finally reached 7,010±360 µg/m^3 of NO_2 at 1,100 ml/min Ar flow (Table I).

The formation of excited NO_X molecules in physical plasma leads to the emission of UVC radiation. Table II shows that increasing NO_2 formation was accompanied by an increased intensity of high-energy UVC radiation in the CAP effluent.

When determining gas concentrations, dilution effects must be expected with increasing distance from the emission source. The NO_2 concentration was thus determined at angles of 40˚ and 90˚ to the longitudinal axis of the CAP effluent at distances of 10, 20, and 30 cm from the CAP effluent (measurement setup, see Figure 1). In this setup, the UVC sensor acted as a baffle to simulate the surface of a treated material or patient. The NO_2 concentrations measured at an angle of 40˚ to the longitudinal axis of the CAP effluent were in the range of ambient air and did not change with increasing distance from the CAP effluent (Table III). In contrast, measurements at an angle of 90˚ demonstrated much higher NO_2 concentration,

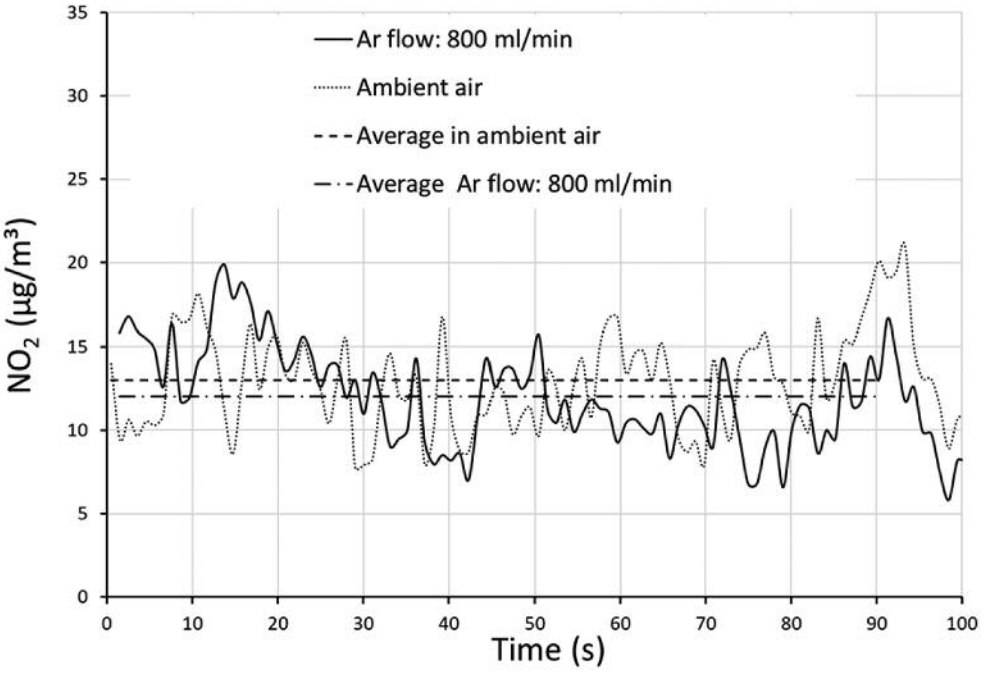

Figure 4. *Determination of the NO_2 ambient concentrations with the cold atmospheric plasma high-frequency generator device switched off and with the Ar flow running using the NO_2-specific I-55D gas sensor (IT Dr. Gambert, Wismar, Germany). The data represent the time course of a representative measurement series.*

Table I. *Determination of NO_2 formation with NO_2-specific I-55D gas sensor (IT Dr. Gambert, Wismar, Germany) at increasing Ar flow rate in the cold atmospheric plasma instrument. The data are given as average values with the device-specific errors as deviation.*

Ar flow rate (ml/min)	NO_2 (µg/m^3)
500	1,450±150
600	1,280±410
700	980±290
800	600±50
900	1,960±350
1,000	4,510±270
1,100	6,710±560

Table II. *Determination of ultraviolet radiation C (UVC) intensity in the range of 200-275 nm with a SUV 20.2 UVC sensor with increasing cold atmospheric plasma mediated NO_2 formation. The data are given as average values with the device-specific errors as deviation.*

NO_2 (µg/m^3)	UVC Intensity (mW/m^2)
850±80	45
1,310±150	56
2,027±130	66
2,480±150	85
2,790±150	90

Table III. *Determination of NO_2 formation with the NO_2-specific gas sensor I-55D (IT Dr. Gambert, Wismar, Germany) on a baffle plate according to angle and distances from the center of the baffle plate of 10 cm, 20 cm, and 30 cm. The data are given as average values with the device-specific errors as deviation.*

Angle (°)	Distance (cm)	NO_2 (µg/m^3)
40	10	23±4
40	20	22±4
40	30	22±4
90	10	478±68
90	20	87±37
90	30	27±6

which decreased rapidly with increasing distance from the contact point of the CAP effluent and the baffle.

Due to its toxicity, NO_2 production must be taken into account when applying CAP for two reasons. Firstly, prolonged exposure to NO_2 may potentially endanger both the patient and the operator. Secondly, among other factors, CAP-generated NO_2 may also be responsible for the biological effect of medical CAP treatment, *e.g.* in oncology.

To address this issue, NO_2 incubation experiments with human cancer cells were performed. CAP treatment of SK-OV-3 ovarian carcinoma cells led to a significant inhibition of

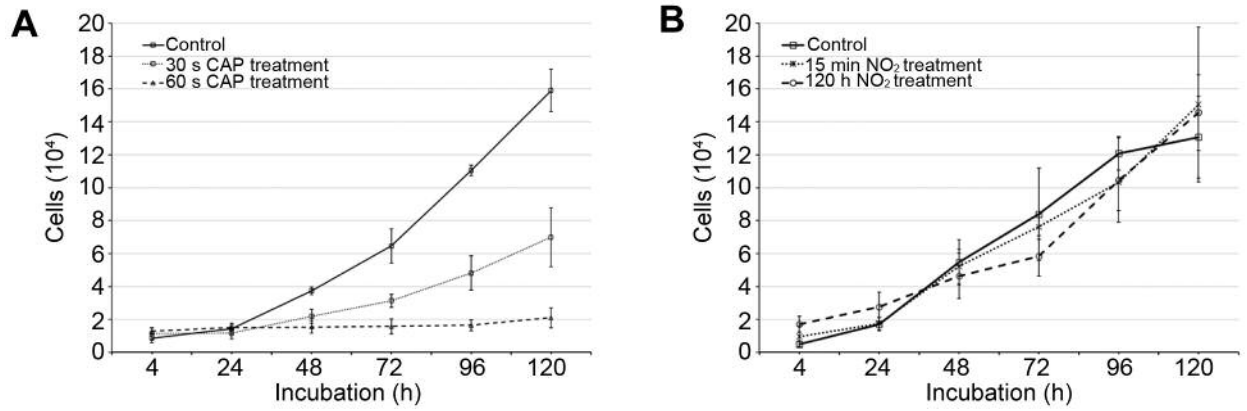

Figure 5. *Growth analysis of SK-OV-3 human ovarian cancer cells over a 120-h period (A) after single cold atmospheric plasma treatment of 30 s and 60 s, and (B) without cold atmospheric plasma treatment but in the presence of 1.925 μg/m³ NO_2. The cell number was determined using a CASY TT Cell Counter and Analyzer (Roche Applied Science, Mannheim, Germany). The data are given as mean±standard deviation.*

exponential cell growth depending on the duration of treatment (Figure 5A). After an incubation period of 120 h, the cell count was reduced 2.3-fold compared to control cells by a single initial CAP treatment of 30 s. With a single initial treatment of 60 s, cell growth was reduced 7.7-fold. To examine whether this growth-inhibitory effect was also mediated by newly produced NO_2, cancer cells were incubated with 1,925 μg/m³ NO_2, and cell growth was determined by cell counting (Figure 5B). A short NO_2 incubation for 15 min corresponding to the NO_2 concentration achieved with CAP treatment showed no effect on cancer cell growth. Even continuous incubation with 1,925 μg/m³ for 120 h did not indicate any growth-inhibitory effects on the cells.

Discussion

By spectral analysis in the UVC range, excited NO was detected during CAP operation. The recorded spectrum was very close to an in silico-simulated NO spectrum (10) and, with a few exceptions in the short wavelength range, matched with maximum deviation of ±0.05 nm. This is the width of one channel of the photodetector, which means that these variations are within the range of the instrument's resolution. However, it was not possible to carry out temperature determination for the molecules, atoms, and their energetic states with the used device, because the resolution was too low (11). The recorded spectra of the CAP source were confirmed by spectral data where a comparable Ar (95%)-N_2 (5%) plasma and a pure N_2 plasma were analyzed (12, 13).

In plasma, N_2, O_2, and H_2O molecules diffusing from the ambient air into CAP effluent are converted into radicals or into excited states by splitting off individual atoms or by ionization (14, 15). The concentrations of the individual reactive species change both temporally and spatially within the plasma. The type and number of species produced depend on the operating conditions of the plasma device (14). Varying humidity in the carrier gas (16) or differences in the electrode length (17) influence the composition of the reactive oxygen and nitrogen species, which makes it challenging to compare different CAP devices.

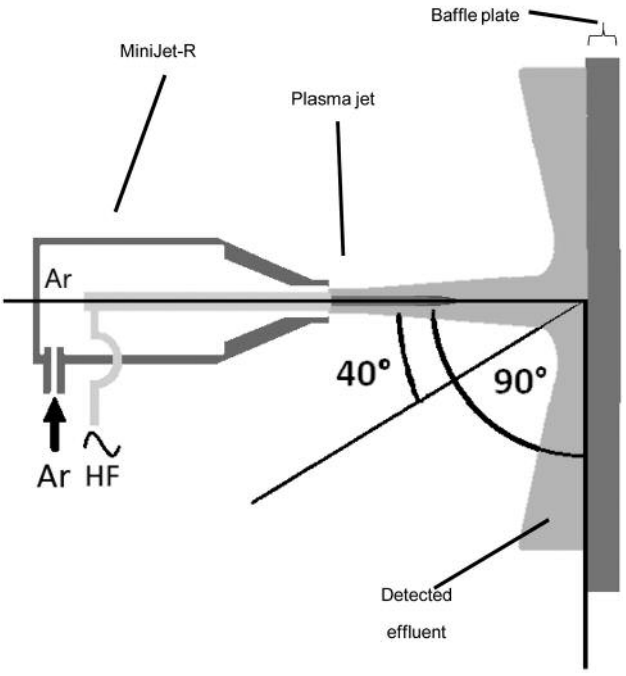

Figure 6. *Circular gas dispersion when a cold atmospheric plasma gas jet (light grey) hits a surface (dark grey) perpendicularly (20). The gas generated at the plasma effluent is transported along with the Ar stream and spreads in all directions along the surface (middle grey). The gas concentration is clearly lower along at a 40° angle to the plasma effluent than at an angle of 90°, i.e., in the immediate proximity of the surface.*

Examinations with the APNA 370 NO_X monitor did not detect NO as predicted by spectral analysis. However, clearly increased concentrations of NO_2 were detected. Since formation of NO in atmospheric plasma has already been described (15), it can be assumed that the newly formed NO was converted very quickly and quantitatively into comparatively stable NO_2 (14, 15). A total of 73 reactions for the degradation of NO are described, and another 87 reactions are described on how NO_2 can be formed from primary reactive oxygen species; 21 reactions alone lead directly to the formation of NO_2 from NO (14).

NO_2 formation was influenced by the operating parameters of the CAP device. With increasing flow rate of Ar carrier gas, the flow velocity of the plasma increases, and, due to the Kelvin–Helmholtz instability of flow interfaces, more intensive turbulence of Ar and ambient air takes place. The increased input of molecules from the ambient air, in turn, enables an enhanced formation of NO_2 (18). The increasing NO_2 synthesis rates also led to an increase in UVC intensity. The measurement of UVC intensity, however, varied widely. This may be due to the technical characteristics of the HF generator. Moreover, particles emitted from the ambient air may disturb the homogeneity of the plasma, leading to disturbances of the NO_2 formation and the UVC radiation emitted in this process (19).

Aspects of application and operational safety are essential points in the characterization of new potential treatment procedures for medicine. With regard to increasing medical indications for CAP, it must be ensured that the formation of toxic agents can be excluded when CAP devices are used. In this context, both regulations for medical devices for the protection of the treated patients and legal regulations for occupational health and safety must be taken into account so that the operators themselves are not harmed. When a gas jet hits a surface perpendicularly, the gas spreads over the surface like a circular disk (20). During this process, NO_2 is transported along with carrier gas of the CAP (Figure 6). When treating patients, any such generated gases might potentially be inhaled by the patient or operator, demanding that concentrations be below the required levels. Depending on the distance to the CAP effluent tip, measurements of the NO_2 concentration at an angle of 90˚ to the longitudinal axis of the CAP effluent showed that concentrations of up to 500 $\mu g/m^3$ NO_2 were generated. However, these concentrations were still below the limit of 950 $\mu g/m^3$ specified in Europe (21). Investigations with tumor cells showed that the experimental conditions did not exert any toxic effect on the cells. A comparable single CAP treatment of the cells of 30 s and 60 s led to strong inhibition of cellular growth. However, CAP-mediated NO_2 emission did not seem to play a role in this. Incubation of the cells with 1,925 $\mu g/m^3$ NO_2 for 15 s, which should be equivalent to a short CAP treatment, showed no effect. Even prolonged incubation of the cells for 120 h showed no evidence of antiproliferative effects of 1,925 $\mu g/m^3$ NO_2 under these conditions. However, it remains an open issue as to whether NO_2 can cause other changes in cells.

In the medical application of HF devices under atmospheric conditions, the formation of toxic gases such as NO or NO_2 must be taken into account in addition to the possible emission of electromagnetic radiation. Before any medical application, appropriate analyses must be carried out and compliance with occupational exposure limits must be ensured. The emission of harmful agents can be minimized in the development phase by optimizing the individual technical components of a CAP device. However, in studies with healthy individuals it was confirmed that NO_2 concentrations from 1.880 to 13.500 $\mu g/m^3$ had no effect on lung function or the O_2 and CO_2 load of the blood (22). Even in patients with asthma, NO_2 concentrations in these ranges did not lead to restrictions in lung function (23). Therefore, it cannot be assumed that the NO_2 concentrations detected when using this CAP device lead to health risks.

Conclusion

The operation of the MiniJet-R CAP device (Heuermann HF Technik) led to the formation of NO_2 via the intermediate stage NO. UVC radiation was also emitted, reaching energy intensities of up to 90 mW/m^2.

Thus, the use of physical plasma in medical applications is potentially associated with both the release of toxic NO_2 and the emission of high-energy UVC radiation. Consequently, the legal regulations for the protection of the workplace (user hazard) as well as for the application safety of medical devices (patient hazard) must be considered. Although no limits were exceeded in the present study, the frequency and duration of CAP treatments must also be kept in mind.

However, *in vivo* experiments with human cancer cells have demonstrated the fundamental efficacy of the CAP device in reducing tumor cell growth. While avoiding the risks outlined above, for instance through gas venting and radiation shielding at the therapy site, treatment with the MiniJet-R certainly represents a promising option for the therapy of cancer.

Conflicts of Interest

The Authors state that there are no conflicts of interest in regard to this study.

Authors' Contributions

KK: Conducted experiments, data analysis, experimental design, layout of the illustrations; LH: Conducted experiments, data analysis; AN: Conducted experiments; FP: Conducted experiments; GK: Conducted experiments; AK: Experimental design, copyediting; SB: Layout of the illustrations, writing the article; AM: Experimental design, copyediting; MBS: Data analysis, experimental design, writing the article.

Acknowledgements

The MiniJet-R was kindly provided by Professor Dr.-Ing. Holger Heuermann (Heuermann HF Technik, Aachen, Germany). Heuermann HF Technik had no influence on the experiments and their analysis, nor was it involved in the preparation of the article.

The Authors would like to thank the Berlin Air Quality Network, who kindly made the measurements with the APNA 370 NO_X monitor (Horiba) possible.

References

1 Wiegand C and Elsner P: Plasma medicine – cold plasma for treatment of skin infections. Akt Dermatol *43*: 339-345, 2017. DOI: 10.1055/s-0043-11268

2 Rehman MU, Jawaid P, Uchiyama H and Kondo T: Comparison of free radicals formation induced by cold atmospheric plasma, ultrasound, and ionizing radiation. Arch Biochem Biophys *605*: 19-25, 2016. PMID: 27085689. DOI: 10.1016/j.abb.2016.04.005

3 Metelmann HR, von Woedtke T and Weltmann KD: Comprehensive Clinical plasma Medicine: Cold Physical Plasma for Medical Application, First Edition. Berlin, Heidelberg: Springer, 2018. DOI: 10.1007/978-3-31967627-2

4 Weiss M, Daeschlein G, Kramer A, Burchardt M, Brucker S, Wallwiener D and Stope MB: Virucide properties of cold atmospheric plasma for future clinical applications. J Med Virol *89*: 952-959, 2017. PMID: 27696466. DOI: 10.1002/jmv.24701 01

5 Hoffmann C, Berganza C and Zhang J: Cold atmospheric plasma: Methods of production and application in dentistry and oncology. Med Gas Res *3*: 21, 2013. PMID: 24083477. DOI: 10.1186/2045-9912-3-21

6 Daeschlein G, Hillmann A, Gümbel D, Sicher C, Podewils S, Stope MB and Jünger M: Enhanced anticancer efficacy by drug chemotherapy and cold atmospheric plasma against melanoma and glioblastoma cell lines *in vitro*. IEEE Transactions Radiat Plasma Med Sci *2*: 153-159, 2018. DOI: 10.1109/TRPMS.2018.2789659

7 Gümbel D, Suchy B, Wien L, Gelbrich N, Napp M, Kramer A, Ekkernkamp A, Daeschlein G and Stope MB: Comparison of cold atmospheric plasma devices' efficacy on osteosarcoma and fibroblastic *in vitro* cell models. Anticancer Res *37*: 5407-5414, 2017. PMID: 28982850. DOI: 10.21873/anticanres.11968

8 Gümbel D, Gelbrich N, Weiss M, Napp M, Daeschlein G, Sckell A, Ender SA, Kramer A, Burchardt M, Ekkernkamp A and Stope MB: New treatment options for osteosarcoma – inactivation of osteosarcoma cells by cold atmospheric plasma. Anticancer Res *36*: 5915-5922, 2016. PMID: 27793916. DOI: 10.21873/anticanres.11178

9 Georgescu N and Lupu AR: Tumoral and normal cells treatment with high-voltage pulsed cold atmospheric plasma jets. IEEE Transactions Plasma Sci *38*: 1949-1955, 2010. DOI: 10.1109/TPS.2010.2041075

10 Luque JC: LIFBASE: Database and spectral simulation program (Version 1.5). SRI Int Rep MP 99(009), 1999.

11 van Gessel AFH, Hrycak B, Jasiński M, Mizeraczyk J, van der Mullen JJAM and Bruggeman PJ: Temperature and NO density measurements by LIF and OES on an atmospheric pressure plasma jet. J Phys D Appl Phys *46*: 95201, 2013. DOI: 10.1088/0022-3727/46/9/095201

12 Foissac C, Krištof J, Annušová A, Martišovitš V, Veis P and Supiot P: Vacuum UV and UV spectroscopy of a N2–Ar mixture discharge created by an RF helical coupling device. Plasma Sources Sciene Technol *19*: 55006, 2010. DOI: 10.1088/0963-0252/19/5/055006

13 Sewraj N, Merbahi N, Gardou JP, Rodriguez Akerreta P and Marchal F: Electric and spectroscopic analysis of a pure nitrogen mono-filamentary dielectric barrier discharge (MF-DBD) at 760 Torr. J Phys D Appl Phys *44*: 145201, 2011. DOI: 10.1088/0022-3727/44/14/145201

14 van Gaens W and Bogaerts A: Kinetic modelling for an atmospheric pressure argon plasma jet in humid air. J Phys D Appl Phys *46*: 275201, 2013. DOI: 10.1088/0022-3727/46/27/275201

15 Schmidt-Bleker A, Winter J, Bösel A, Reuter S and Weltmann KD: On the plasma chemistry of a cold atmospheric argon plasma jet with shielding gas device Plasma Sources Sci Technol *25*: 015005, 2016. DOI: 10.1088/0963-0252/25/1/015005

16 Winter J, Wende K, Masur K, Iseni S, Dünnbier M, Hammer MU, Tresp H, Weltmann KD and Reuter S: Feed gas humidity: A vital parameter affecting a cold atmospheric-pressure plasma jet and plasma-treated human skin cells. J Phys D Appl Phys *46*: 295401, 2013. DOI: 10.1088/0022-3727/46/29/295401

17 Bin Y, Li L, Liu YL, Ge YF, Liu L, Ma N, Le Y and Lin FC: Impact of wire electrode length on nanosecond-pulse diffuse discharge in atmospheric pressure air. IEEE Transactions Plasma Sci *42*: 2492-2493, 2014. DOI: 10.1109/TPS.2014.2309996

18 Iseni S, Schmidt-Bleker A, Winter J, Weltmann KD and Reuter S: Atmospheric pressure streamer follows the turbulent argon air boundary in a MHz argon plasma jet investigated by OH-tracer PLIF spectroscopy. J Phys D Appl Phys *47*: 152001, 2014. DOI: 10.1088/0022-3727/47/15/152001

19 Kossyi IA, Kostinsky AY, Matveyev AA and Silakov VP: Kinetic scheme of the non-equilibrium discharge in nitrogen-oxygen mixtures. Plasma Sources Sci Technol *1*: 207-220, 1992. DOI: 10.1088/0963-0252/1/3/011

20 Richter F and Leder A: Wechselwirkungen runder Düsenfreistrahlen mit ebenen Wänden. Fachtagung "Lasermethoden in der Strömungsmesstechnik" 5. - 7. Sep 2006, Braunschweig, Germany.

21 Bundesanstalt für Arbeitsschutz und Arbeitsmedizin. Technische Regeln für Gefahrstoffe 900 (TRGS 900) – Arbeitsplatzgrenzwerte 1/2006: 46, 2006.

22 Beil M and Ulmer WT: Effect of NO_2 in workroom concentrations on respiratory mechanics and bronchial susceptibility to acetylcholine in normal persons. Intl Arch Occup Environ Health *38*: 31-44, 1976. PMID: 977150. DOI: 10.1007/bf00378318

23 Linn WS, Solomon JC, Trim SC, Spier CE, Shamoo DA, Venet TG, Avol EL and Hackney JD: Effects of exposure to 4 ppm nitrogen dioxide in healthy and asthmatic volunteers. Arch Environ Health *40*: 234-239, 1985. PMID: 4051580. DOI: 10.1080/00039896.1985.10545925

Received March 9, 2020
Revised April 6, 2020
Accepted April 8, 2020